The effect of local wind and waves on the areas of reduced risk BONUS BalticWay Deliverable 4.3

Jens Murawski, jacob Woge

Contents

1 Introduction

Oil is a toxic chemical substance that when handled in large quantities at sea, puts the marine and coastal environment at risk of being rendered severely polluted or inhabitable for a considerable span of time. Oil may be released into the environment from

drilling (production) platforms, from pipelines, or from vessels. An oil spill is usually the consequence of some sort of accident. It may take place abruptly, or during an extended time span, potentially of the order of months.

Many oil spills result from transporting oil at sea. The size of spills originating from a vessel varies several orders of magnitude, depending mainly on whether oil is the cargo itself, or just the vessel's driving agency. In the first case, several hundred thousand tonnes of crude oil may be lost to the environment, in the second case, of the order of 1,000 - 10,000 tonnes of refined (fuel) oil. Since a vessel contains a limited amount of oil, spills from vessels are often, but not always, of relatively short duration, and can sometimes be regarded as instantaneous. The impact on the environment, however, may last for decades.

Oil spills are most efficiently combated at sea, before any shoreline is polluted. If weather conditions are favourable, barricades may be set up to contain the spill, and oil is collected (pumped) from the sea surface or combated chemically. At the coast, conditions for combating are usually less perfect, and a major clean-up operation is commonly at hand. Prevailing weather conditions, and the distance from spill site to shore, are the major factors deciding which scenario (open water or coast) unfolds.

Minor spills disperse into the open waters, provided time enough is given before the bulk of the spill goes onshore. In semi-enclosed seas like the Baltic, the cumulated effect of such spills are detectable as a background hydrocarbon concentration (Pikkarainen et. al. [2005]). Still at a moderate level, this diffusive pollution is considered less harmful than soiling the ecologically sensitive shoreline.

1.1 Rationale and methodology of oil drift and fate modeling

Oil spill modelling is a valuable tool for combating oil spills, and has been so for about thirty years now. With time-dependent information on the oil's location, slick size, spreading, composition, and drift preventive measures can be taken if met-ocean conditions allow it. The standard oil drift model produces this kind of information, and is used as an operational stand-by tool. The single emergency (or drill) drift calculation is performed in real time in order to track a spill taking place at a given point or limited span in time and space, with the weather and ocean conditions that happen to be at hand, now and some days into the future.

In this chapter a matrix of drift calculations is carried out, studied and analysed statistically. This includes a) a surface mesh of spill locations covering the area of interest (Gulf of Finland), and b) an exhaustive set of analysed met-ocean conditions, including complete seasonal variations. The resulting statistical description of the spill trajectories originating from each individual spill site gives way for a comprehensive risk analysis: which sites or areas are less prone to present a risk of contamination of any shoreline within 'striking distance' of the spill. Since from the drift model's perspective, oil never disappears from the environment, and will very probably hit upon a coast eventually, the risk is quantified in two ways: a) as the number of days until first shore contact, and b) as the fraction of the spill that will reach any shore within a fixed time frame.

The risk of shore contamination from a given area is thus specified solely by a large number of weather and circulation driven Lagrangian drift trajectories. Other features of oil's chemistry and physics, collectively termed weathering processes, are taken fully into account when carrying out the simulations, but do not constitute part of the result analysis.

One obvious drawback of this method is that a spill is supposed to take place with the same likelihood, independent of geographical position or weather conditions. In reality, some weather and ocean conditions (high winds and waves, fog, sea ice, and – in other parts of the world – icebergs) are riskier than others, and some waters are more difficult to navigate than others. Merging sea traffic towards the same pathways would in itself enhance risk of collision. It is, however, considered beyond the scope of this work to introduce site- or weather-dependent weights to each spill simulation.

The risk map resulting from a statistical analysis of a large number of hypothetical spills makes it possible to identify ecologically safe pathways though the body of water examined, by minimizing the cumulated risk along the ship track, and taking further into account that the time spent at sea (track length) presents a risk in itself.

1.2 Layout of this chapter

This chapter falls in three parts. First, basic features of (operational) oil spill modelling are described in some detail, with basis in one specific model as example. Focus is on the features that are assumed to cause differences to the reduced risk area design based solely on Lagrangian drift simulations. Second, the concept of sea way design is introduced, including a cross-evaluation of the ecological and economic factors influencing ship routeing. Finally, the Gulf of Finland is used as an example of utilising oil drift modelling to identify ecologically safe sea ways.

1.3 Oil drift models

An oil drift or spill tracker model simulates hypothetic or real oil spills. Given an exhaustive description of the spill itself (time, location, magnitude, duration, oil type), and prevailing and upcoming wind, wave and current conditions, the modelling effort aims to calculate as accurate as possible the state of the spill at future times. This includes the geographical extent of the spill, where and when oil will drift onshore, oil composition, toxic levels and slick layer thickness. In hindcast mode and/or scenario studies, such calculations assist in risk analysis and assessment. In forecast mode, the information provided by an oil drift simulation serves primarily as a decision tool for spill response: how to combat a spill and reduce the environmental impact. Sensitive regions at risk may be identified and defended by deployment of barriers at sea. Oil may be combated chemically or pumped, depending on slick thickness, chemical status and the amount of spreading.

The basis for oil drift simulation, or spill tracking, is the Lagrangian trajectory. The simple displacement-with-time calculation $\underline{s} = \int_{t_1}^{t_2} \underline{u}\, dt$ applies well to floating or (partially) submerged objects. For sake of simplicity and calculation speed, the same method

is applied to chemical substances or pollutants. The pollutant is treated as a particle, that drifts passively with the ocean current. A particle resembles an object in the sense that it cannot be split, but has inherent properties that can change with time, like shape and size. A particle position is updated by the simple time-stepping algorithm above, with proper representation of the advection velocity u. Since inaccuracies accumulate along the particle track, high-precision methods and/or high time resolution (of the order of ten minutes) is required in such calculations.

When the pollutant stems from a point or a line source, with limited time duration, the Lagrangian trajectory calculation is orders of magnitude more efficient than a Eulerian approach in determining pollutant concentration levels attained. Apart from general water properties, the latter method is used to simulate spreading from more or less permanent point sources, e.g. river outlets which (potentially) in time influence the entire body of water considered. A Eulerian advection calculation of, say, salinity or nutrients, gives complete concentration maps as a direct result. The Lagrangian method, in which the computational effort is limited to the region actually affected, requires a post-processing step to transfer drift model results (particle position) into concentration (toxic) levels. The study presented below is basically a trajectory analysis, so this second step is not carried out.

The Lagrangian trajectory is purely advective-deterministic. Commonly, an ensemble of trajectories is calculated, with some (pseudo-random) perturbation method applied to the forcing fields (ocean current, wind, waves), the spill site, or the spill time. The resulting trajectory ensemble is represented at a given instant by a particle "cloud". For object tracking, the trajectory ensemble may be interpreted as a probability distribution. For substances, the ensemble is commonly interpreted as representing natural spreading or even splitting up of the spill as particles separate from each other, by processes not resolved by the basic forcing fields. For instance, a spilled substance will slowly spread isotropically with time as $\sqrt{t}$, even in total absence of external forcing, due to Brownian motion. Each trajectory is regarded as deterministic in its own right, pertaining to a fraction of the spill or a certain amount of spilled substance. Again, the Lagrangian approach reduces the ensemble prediction method to a manageable size in real-time applications, where calculation speed is a major issue. Only along trajectories do we need to perturb the advection velocity. While full met-ocean model ensembles have e.g. of the order of 20-50 members, trajectory ensembles produced by drift models are typically at least an order of magnitude larger.

As an example, in S.Dick et al.[1990] the perturbation of the forcing fields is handled by carefully scaled random contributions to the advection velocity, which in turn is composed as a vector sum of three-dimensional ocean current, wind drift (typically attaining 3% to 3.5% of the wind speed at the surface, and decreasing logarithmically with depth), and an additional non-isotropic horizontal particle spreading velocity, which depends on wind velocity and acts to elongate the particle cloud in the wind direction.

For inactive substances of neutral buoyancy (a colour agency, a radio-active tracer, etc.), the method described above is sufficient to describe the time evolution of a spill. Different from many other pollutants or tracers, oil in sea water is a chemically and

physically active substance, interacting both with sea water, air and (suspended) sediment, reacting on sunlight, impacting the biological environment, and, on a longer time scale, being impacted through biodegradation. These interactions makes the oil undergo transformations by altering its composition, and thereby its chemical and physical properties.

Superstructures to simulate short-to-medium time range chemical processes collectively termed 'weathering', spreading (horizontal and vertical), and buoyant motion are built upon the advective-deterministic approach. This superstructure feeds back on the advection process, mainly through oil's ability to reposition itself vertically in a water column with vertical current shear. Changes in density influence the buoyancy relative to sea water, while viscocity changes influence the spreading process and oil's ability and tendency to form a thin surface film. When part of an oil spill is mixed down (or released at depth), it moves at a different speed and direction than oil at the surface. This mechanism may elongate and even split up a spill in a number of isolated patches, as the submerged part of the spill lags behind oil at the surface.

With this formulation, an oil particle is represented by a state vector with information about chemical composition and physical state, i.e. geographical position, volume, and shape (area and thickness). When oil is present in the shape of a surface film, it spreads by advective-diffusive processes mainly horizontally, in two dimensions, while vertical spreading is governed by buoyancy forces and wave-induced mixing. This makes it appropriate to assign to an oil particle a disc-like shape, defined by radius or area, and thickness. The 'cloud' of particles constitutes the whole spill. Particle state vector summation and averaging gives information about general spill state: total volume, mean thickness, average position and composition.

When an oil particle sinks to the sea bed or reaches the shore, it is assumed to leave the water phase. All processes come to a halt as the particle settles and reaches the end of its trajectory.

Similar Lagrangian/particle methods, with a chemico-physical superstructure built upon a basic advection method, are used in atmospheric pollution modelling, simulating e.g. three-dimensional spreading of radioactive substances or volcanic ashes (Sørensen et al. [1998], [2007]). Again, the spill is split into a number of non-interacting particles, each representing a certain amount of pollutant or fraction of spill, and each particles displacement and evolution is tracked in time (Sørensen et al. [2007], Dick et al. [1990]). This has proved valuable in several incidents with large-scale impact and duration of weeks to months (Tjernobyl and Fukushima accidents (1986, 2011), Eyjafjallajökull eruption (2010)).

In a real-time oil spill simulation, information about the amount or rate of oil spilled is often incomplete and based on rough estimates. The oil composition is unknown or imprecise, for instance limited to the basic distinction between refined (fuel) oil and unrefined (crude) oil. Ambient sea water density and temperature are often estimated from climatology, and taken to be constant. Sea ice and wave conditions may be unknown or parameterised. Trajectories may still be calculated with a sufficient degree of accuracy, but the description of chemical and physical evolution of the spill, important for oil

combating, may suffer as a consequence.

Oil is composed of a large variety of hydrocarbon compounds, ranging from from light, volatile kerosene, to heavy, stable tar. The exact composition constitutes an oil type. The possible number of crude oil types is almost infinite (Børresen [1993]). The composition can be determined by spectral analysis, equivalent to taking the finger print of that particular oil type. For simplicity, in oil drift models hydrocarbon compounds are grouped into fractions, defined by chemical structure and molecular weight. The relative weight of each fraction determines distillation properties, density, saturation vapour pressure and viscosity at a reference temperature. The initial composition constitutes a model oil type, typically an approxmation to a known crude oil or a refined (fuel) oil. The density of the oil is the weighted mean of the density of each compound. The composition and the physical properties of the oil, changes with time due to weathering processes. Volatile components (kerosene) quickly evaporate if oil is exposed to air. This process takes of the order of half a day. On a slightly longer time scale, of the order of two days, oil mixes with sea water under the action of surface waves to form a stable emulsification. In the mixture, the water content is two to four times larger than the oil content, and the viscocity increases several ordes of magnitude. The consequences for the combating effort are volume increase and changes in fluid properties (affecting the pumping), which must be taken into account.

Weathering processes both affect and depend on the chemistry of the oil. Only some of these processes are treated operational oil drift models: evaporation, water-in-oil emulsification, spreading and horizontal and vertical dispersion. More elaborate methods include oxidation, dissolution, interaction with suspended matter and others. For a comprehensive review, please refer to S. Dick et al. [1990], Børresen [1993] and Reed et al. [1999].

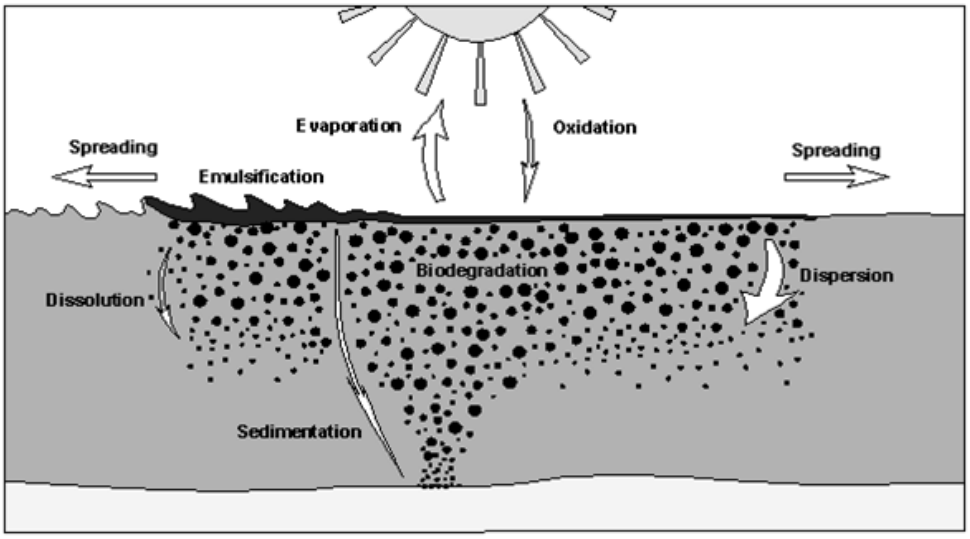

Figure 1: Weathering processes (http.//www.itopf.com/fate.html)

Spreading is an an-isotropic process, with different mechanisms responsible for horizontal and vertical spreading, respectively. It is important for the early stages of an oil spill as well. An oil slick spreads horizontally in three phases until a terminal thickness is reached. Still regarding an oil particle as a circular disc, the initial spill radius r first increases by buoyancy-inertia forces, then, as the slick grows thinner, the spreading moves into a buoyancy-viscous regime, and the final stage is governed by viscosity and surface tension (Fay [1971]). The oil slick thickness decides which spreading phase is active. The last two phases depend strongly on oil viscosity, i.e. oil composition and ambient temperature. The ability of oil to form a quasi-stable emulsification with sea water, with viscosity increase of several orders of magnitude (Børresen [1993]), plays a key role in these processes. One cubic metre of oil is spread over $0.1km^2$, so that the terminal slick thickness is just a few tens of microns, depending on emulsification.

The vertical spreading consists of downward mixing due to upper-layer turbulence, generated by surface waves, and buoyant rise, making the oil resurface in absence of turbulence. The mixing depth may be parameterized as dependent on wave height or wind speed. When a surface slick is mixed down, it pollutes the upper layer uniformly down to the mixing depth. For example, if an oil slick of thickness 10μ with zero water content (corresponding to a volume of $10m^3/km^2$) is mixed down to 10m depth, the resulting concentration is $1,000ppb$ total hydrocarbon (TH).

Oil spill modelling in ice covered water is not widely described in the literature, at least not to our knowledge. The wind-drift is reduced in the presence of sea ice depending of the ice concentration. The process is discussed in Johanson et al. [2005], where sea ice influences oil drift in dense ice (ice concentration larger than 70%) while there is no influence in low ice concentrations (less than 30%). For oil at the surface, the drift velocity is a combination of current speed and ice drift velocity, with proper weights assigned depending on ice concentration. This is a rather crude approach, limiting the effect on the ice to the drift velocity. Weathering processes are significantly slower in ice leads, but the spatial scale is of the order of meters, typically not resolved by a numerical ice model M.Reed et al. [1999]. This is an unresolved key problem.

Oil drift and fate modelling as described above has been developed largely since the 1980'ies, and many models are now on the market. Differences in forecasting quality may be large, but are mainly related to externalities, such as differences in model set-up and forcing. Statistical results of drift pattern analysis and ship routing design studies are expected to be resilient to the choice of the oil drift and fate model. The model that has been selected is the operational oil dispersion model BSHdmod Dick et al. [1990]. It has been developed by the Federal Office for Sea Shipping and Hydrography (BSH) for the German Bight and has been applied to the North Sea and Baltic Sea by the Danish Meteorological Institute (DMI) and BSH. A comparison of different oil drift and fate models is not intended.

DMI's oil drift model has been developed for tidal dominated seas like the North Sea, with strong waves, shallow near coastal waters and limited impact of sea ice on oil drift and fate. The model has been successfully applied to the Baltic Sea, which is partially ice covered for most of the year, using basic assumptions about the dependency of oil

dynamics on sea ice.

2 Environmental risk assessment

2.1 Introduction

The ever-increasing density of maritime traffic and especially tanker traffic contributes strongly to the possibility of shipping accidents with the consequence of near-coastal oil spills. Model based investigations of risk factors have been used successfully to minimize the consequences of shipping disasters and to increase the efficiency of sea way designs. Economical and environmental factors are thereby fundamentally non-conflictive. In the process of making shipping routes safer and environmentally friendlier by adaptive design, they often become more beneficial in terms of faster travels (going with the currents instead of against them) and lower fuel consumption. Environmental and economical considerations are rarely entering the planning stage of sea way designs. Model developed design criteria can contribute to optimized sea traffic, by effective route planning, emission reduction, improved disaster management and increased performance of transport vessels.

The developed BalticWay technology addresses the problem of a combined assessment of environmental and economical factors in two main steps. Firstly, optimum environmental fairways are identified that favour semi-persistent current pattern with flow characteristics that propagate oil spills off-shore with the effect of a substantial increase in combating time. Secondly, the emerging fairway designs are evaluated under economical viewpoints using a classical ship routing system. Outcomes are certain numbers of alternative ship routes with characteristic risk and economical factors. The combined evaluation identifies optimum fairways with increased oil residence time at sea, reduced probability of coastal oil landings, faster sea travels and reduced amount of fuel consumption.

With independent model platforms of atmospheric, wave and ocean circulation models for the Baltic Sea and the Gulf of Finland, disaster impact model for the drift and fate of pollutants at sea and ship routing and performance analysis service, the BalticWay project consortium is in the unique position to evaluate sea way designs under safety, risk, disaster impact and ship performance viewpoints. Independent evaluations contribute to the informative value and the significance of consistent project findings.

BalticWay aims at a substantial reduction of ship-caused environmental impacts by reducing the risk of oil spills as a function of the cost of the consequences. Model based investigations of the semi-persistent and statistically significant current patterns and oil drift characteristics are used to assess the environmental potential of adaptive sea way designs. Existent heterogeneous current and oil drift pattern make it possible to design ship routes with statistically lower possibility of cost intensive near coastal oil hits. The model analyses focus on the Gulf of Finland and is based on extensive wind, wave, ocean circulation and oil drift studies.

2.2 Models

Model based investigations of oil drift pattern involve two kinds of simulations: high-resolution weather and ocean circulation model runs for forcing fields and oil drift and fate model runs for drift assessments. Currents and winds drive oil advection and affect oil chemistry and physics in sea water due to weathering. The model runs with meteorological forcing from Denmark's Climate Centre (DKC) 50 years reanalysis (1960 to 2010) (Christensen et al. [2006]) for the North Atlantic, North Sea and Baltic Sea. Hourly forcing in 0.11 degrees resolution is available. For ocean circulation simulations Denmark's Meteorological Institute's (DMI's) operational circulation model (appendix1 [2.6]) for storm surge warning and ocean forecasts is used. The set-up covers the North Sea, Baltic Sea in 5km resolution and the transition zone in higher resolution of 1km. An additional 1km Gulf of Finland grid was two-way nested into the Baltic Sea grid in order to model 3D ocean currents in high spatial resolution for oil drift simulations. Circulation studies in the Gulf of Finland (Oleg Andrejev et al. [2011]) show that 1km is an adequate resolution for the simulation of essential ocean current features, of which the sub-surface Neva river outflow in 3m to 10m depth is the most prominent one. To account for this, the vertical model resolution in the upper 10m of the Gulf of Finland model is set to 3m at the surface and 1m below. In the North Sea and Baltic Sea, 8m surface and 2m sub-surface levels are used to include the amplitudes of the tides and surges. Below 10m the vertical resolution varies gradually from 2m in the upper 80m to 25m at 125m depth, the largest depth in the Gulf of Finland. Below 125m the layer thickness increases to 50m at 550m in the Norwegian rim. The model is forced by tidal sea level composed of 17 constituents and pre-calculated surges at the open model boundary to the North Atlantic. Salinity and temperature boundary conditions from POLCOM monthly climatology and daily river data from SMHI's hydrological model have been used (Bergström [1976], [1992]). The run was initialised with operational archive data in August 1990 in order to avoid ice in the Gulf of Finland. The increase in spatial resolution (the operational model has the same resolution as the North Sea and Baltic Sea set-up) made a model spin-up over a period of little more than one year (until the end of 1991) neccessary, to ensure that the density field is in balance with the velocity field. The following years 1992 to 1994 were selected for the oil drift and fate model studies.

Oil drift and fate simulations employ DMI's operational model, which has been developed by the Federal Office for Sea Shipping and Hydrography (BSH) [1990] for the German Bight and has been successfully applied to the North Sea and Baltic Sea. The model deals with ship driving fuel oils and varieties of naturally occurring crude oils. The classes range from extra heavy and heavy crude oils (IFO 450, Crude Venezuela) with high solidification points and low evaporation, heavy fuel oils (Bunker C), conventional crude oils (Crude Statfjord, Crude Ekofisk, Crude Nigeria), light crude oils (Crude No. 2) and light volatile petroleum products with high evaporation (Kerosinee). Each oil class is composed of 8 fractions with different boiling points and molecular weight. For the Gulf of Finland simulations conventional crude oils (Crude Statfjord) was selected. Oil in sea water undergoes several transformations. DMI's model considers atmospheric

interaction processes (evaporation), wave dependent ocean surface processes (water-in-oil emulsification), horizontal dispersion and spreading of oil and sub-surface processes (vertical dispersion). Evaporation is treated fraction-wise as a function of mass, molecular weight, vapour pressure and wind velocity according to Audunson [1980] and Dippner [1984]. More volatile fractions eventually evaporate completely. The loss in oil mass is compensated by water-in-oil-emulsification which depends on winds, i.e. waves and is modelled as a saturation process leading eventually to a maximum uptake of 70% of water (Mackay et al. [1982, 1983]). Oil slicks in sea water undergo spreading, dispersion and advection due to currents and winds. Turbulent motions are implemented as random processes. Spreading increases the ratio of covered area to thickness and is driven/balanced in the early stages by gravity/inertia and in the later stages by surface tension/viscosity. It is modelled using modified Fay equations [1971] where spreading in wind direction (wind velocity $\underline{w}$) is enhanced, i.e. spill radius in wind direction is $1 + 0.5 \cdot \underline{w}$ times larger than the radius in orthogonal direction. Additional to spreading, oil parcels are moving with currents (current velocity $\underline{v}$) and winds, whereas an Eulerian scheme $\partial s = v \cdot \partial t$ is employed and 3.0% of the wind velocity in the direction of the wind is added to $\underline{v}$ (Reed et al. [1994]). Horizontal dispersion and turbulence is treated as a sub-grid process by adding to $\underline{v}$ a random component $R \cdot \underline{v}$ and Brownian motion RB. Vertical dispersion is modelled as interplay of upwards buoyant motion according to Stokes law and wave induced downwards mixing, treated as turbulent diffusive process with wind (wave) dependent eddy diffusivity (Sverdrup et al. [1942], Leibovich [1975]). Turbulence effects are included as random droplet size distributions of buoyant oil parcels (Johansen [1982], Forrester [1971]) and random contributions to the eddy diffusivity. Submerged oil parcels are staying submerged in most cases and are stranding at the sea bottom. These parcels are removed from the calculations and are not entering the drift analysis. Considered are only near surface oil parcels that are reaching the shoreline.

2.3 Methodology

Several technologies have been developed for the identification and characterisation of risk optimized fairway designs. These are based on the definition of characteristic, transport related risk factors with well defined optimum values. Optimum fairways are connecting spatial points with low risk in terms of probability of near coastal oil landings and effectively increased combating time (also referred to as residence time at sea). The anisotropy of transport pattern in many sea areas make these factors a complex function of topography and flow regime, i.e. they are not just geometrical functions depending on the distance to the shoreline. Consequentially they are varying with the year and the season, making a statistical approach necessary. A large numbers of pollutant transport simulations have been performed and analysed. The results are statistically significant distributions of characteristic environmental risk factors in space.

Fairway design and evaluation technologies base on four fundamental steps (a, b, c, d). Step number one (a) includes realistic atmosphere and three-dimensional ocean circulation modelling. Pollutant transport due to currents dominates the sub-surface regime

and is at least of the same order of magnitude as wind induced transport at the surface. Step number two (b) involves a multiplicity of pollutant transport and fate simulations for the statistic evaluation of characteristic drift pattern. "Baltic Way" provides the user with a manifold of comparable technologies and possibilities to evaluate the data and ship routing designs under different viewpoints. Pollutant transport has been studied by means of Lagrangian particle drift assessments, where each particle represents a drifting volume of contaminant, has been investigated by passive Eularian pollutant density advection studies and has been analysed by means of operational oil drift and fate model studies. Oil release positions on a medium resolution grid were selected for drift studies in the Gulf of Finland. At the northern side of the Gulf where the drift pattern are expected to favour outflow conditions and westwards transport the release positions were chosen to lay on a latitude x longitude grid of $\approx 3 \times 22km$, whereas at the southern side a lower resolution $\approx 6 \times 22km$ was selected. Fairway design studies base on high resolution lagrangian surface drifter experiments (Soomere et al. [2011a], [2011b], [2011c] [2011d], Xi et al. [2012]) where water parcels were substituted for oil particles and wind and wave effects were neglected. In the framework of this study realistic oil drift and fate simulations are used to evaluate the earlier results and to estimate the effects of oil weathering, winds and waves. For this, characteristic drift measures, i.e. residence time at sea and probability for coastal landings are calculated in (c) step number three. The final step (d) includes the analysis of the results of (c) and therewith the synthesis of all four steps of fairway design generation and evaluation.

2.3.1 Oil drift and fate model studies

The drift and fate of oil in sea water depend strongly on wind and wave conditions and wind and current induced transport. The quality and resolution of the forcing data is crucial for oil predictions, especial in near coastal waters. Special focus was put on the accurate moddelling of the atmospheric and hydrodynamic conditions in the Gulf of Finland. A period of three years: January 1992 to December 1993 was selected for the model based study of oil drft pattern and the evaluation of ship routing designs. The analysis is based on two parameters, the oil residence time at sea and the probability for coastal oil contermination. Modelled are the tracks of continuous oil volumina, associated with passively advected particles. Landing probability is the ratio of released to landing particle numbers. As a statistical measure it is well defined for an ensemble of oil spill simulations. The residence time of oil particles at sea is associated with the time between release and landing and is at the outset a specific measure for an individual oil spill. A characteristic measure for an ensemble of oil spills has to be constructed.

Figure (2) demonstrates the method that was used for the oil drift and fate model based estimation of oil residence time at sea. Pictured are three histograms of the time spent at sea between oil release at three positions and the shoreline landing. The picture represents nearly 100 simulations (for each of the 3 points and for the years 1992 to 1994) of 10 days periods after oil release and includes for each simulation the release of 1000 particles. The simulations are evenly distributed over the seasons with a legging time of 4 days. The oil drift and fate model tracks the trajectory of each particle until it leaves the

Gulf of Finland or hits land. Every landing particle in a depth above 0.5 m is counted. This excludes sea bed fixation and ensures that only near coastal conterminations are studied. The analysis of the residence time at sea focuses on the identification of cluster points, i.e. times at which large numbers of particles land. For each release position, the first peak in the histogram has been chosen to represent the typical residence time of oil at sea. Counting 8 drift simulations per month, for a period of 3 years and for 528 release positions, thus more than 150 000 drift simulations form the basis for the here presented oil drift and fairway design analysis.

Fair way assessments base on constructed measures of oil landing probability and residence time at sea. Favorable fair way designs make intelligent use of the structure of low probability and long residence time domains.

2.3.2 Oil drift and fate model based assessments of characteristic drift pattern and study of their implications for possible fairway design

In its essence the problem of deriving optimum fairways from model results is an inverse one. The accessible information of oil residence time in open waters and coastal hit probabilities for individual runs under specific conditions is related to global distributions of risk parameters and cost functions $\phi(\underline{x}, t)$ for the optimisation procedures. The output are pathways of low accumulated risk specified by path integrals of $\phi(\underline{x}, t)$ which are identified as optimum fairways. Although the cost functions are specified by statistical ensembles of model results and derived risk measures, the fairways are not only connecting local risk minima, but are also optimizing the path length. Longer ship tracks are not only fuel and cost intensive, but also less environmentally preferable, because of intensified ship emissions. Furthermore, longer pathways represent a risk in themself, as the time spent at sea increases. Optimum routes combine minimums of path length and path integrated risk values. This sort of problem is typically approached by Monte Carlo techniques. But the straight forward use of Monte Carlo methods with combined risk and path length cost functions is less promising because of the difference in nature of the two parameters. Risk minimization tends to connect local minima and to produce meandering tracks, whereas path length minimisation tends to generate straight lines. Optimum cost functions that combine the two characteristics could not be found. For that reason, a sequential Monte Carlo approach is used, where the first priority is to minimize the cost function and the path length minimisation is of secondary order. This way risk factors and the pathway length do not have to be weighted against each other, during a optimisation cycle. The optimized cost function at each release position $\underline{X}$ is a constructive measure of the relative time spent at sea $T(\underline{X})/TM$ (runtime of the drift simulations $TM = 10\ days$) and the probability for coastal oil landings $NL(\underline{X})/NT = \sum_r^{nr} NL_r/(nr \cdot 1000)$ (number of releases nr, number of oil particles per release 1000). Ad-hoc weighting factors $f_1 = 2$ and $f_2 = 1$ are introduced to strengthen the relative significance of oil combating time to landing probability. This way, the possibility of successful oil combatting is weighted against the severeness of an oil spill, as

the probability factor refers directly to the amount of oil that is reaching the shoreline.

$$\phi(\underline{X}) = \frac{f_1}{f_1 + f_2} \cdot \frac{T(\underline{X})}{TM} + \frac{f_2}{f_1 + f_2} \cdot \left(1 - \frac{NL(\underline{X})}{NT}\right) \tag{1}$$

In a first step, $\phi(\underline{X})$ is spatially interpolated to $\phi(\underline{x})$ to increase the resolution ($\underline{\mathrm{x}}$ marks all model grid points) and random sampling of $\phi(\underline{x})$ along paths $p(\underline{x})$ is used to minimize the path integral of $\phi(\underline{x})$ along p($\underline{\mathrm{x}}$). The paths $p(\underline{x})$ are initialised with lines connecting the maxima of $\phi(\underline{x})$ at the longitudes of the release grid. The optimisation during the first phase focused on the maximisation of the cost function and is using regular random re-initialisations to avoid local minima of $\phi(\underline{x})$ and simulated anneeling to gradually restrict the random modifications and to freeze the pathways into their final configuration. The results are often complicated fairways, unsuitable for navigation. That is why in a second step, the length of a pathway is minimised. To avoid straight lines as solutions, random positions along the pathways in regions where the cost function $\phi(\underline{X})$ is at least 0.7 were randomly chosen to remain fixed. Monte Carlo techniques use random variations that follow the spatial grid representation of the circulation model $\underline{x}$ to find a global minimum of the path length. At each model longitude the pathway is pseudo-randomly shifted in lattitude direction. Pseudo-randomly means here, that going eastwards the random shift happens in a latitude environment of the western neighbour point. The resulting optimum pathways maximise the value of the integrated coast function and minimize the path length. It should be mentioned that the optimum can not be absolute, but has to remain relative. That means, that an optimum pathway is only characterised by the ratio of its global cost function to the corresponding cost function of other path ways. Criterium is the maximisation of Ψ, the integrated local cost function along paths $s(\underline{x})$.

$$\Psi = \frac{\int \phi(s(\underline{x}))\, ds}{\int ds} \tag{2}$$

2.4 Results

Oil drift patterns at the sea surface are subject to seasonal variations and depend strongly on dominant meteorological conditions and riverine transport. Below the surface, wind drift is reduced and currents play the major role in oil advection. The result is a strong seasonal variation of the mean drift pattern, drift velocities and distribution of oil landing positions at the coast. Buoyancy is often unable to overcome wave induced downwards mixing at later stages of the spill evolution when weathering has removed the more volatile and dissolvable oil components. Submerged particles remain submerged in most of the cases and as only particles at the surface (depth $< 0.5m$) are counted, are therefore removed from the analysis. In the Gulf of Finland, the dominant driving force for oil drift advection from offshore locations is winds during stormy seasons and are the currents during calm seasons. It could be argued, that 3.0% of the wind speed in the direction of the wind (Reed et al.[1994]) is to high a value for the oil wind drift in semi-enclosed regions like the Gulf of Finland. The value was estimated on the basis of drift experimants under off-shore conditions. It was found that the value holds for

light winds and non-breaking waves, conditions that are typical for the Gulf of Finland. Furthermore, wind drift fractions of around $3 - 3.5\%$ are used for operational oil drift prediction in many different seas. The range of percentage values that can be found in literature cover 0.8% to 5.8% (Pahlke [1985]).

The Gulf of Finland provides a good example for drift model based investigations of characteristic oil drift pattern. Situated at the north-eastern extension of the Baltic Sea, the gulf is a semi-enclosed sub-basin with a strong salinity gradient, supported by the Baltic Sea in the west and the largest regional fresh water source, the Neva river in the east. Its main circulation is strongly wind driven, but density driven currents play as well a role (Andrejev et al. [2004]). Wind driven inflow at the Estonian side and fresh water outflow, supported by the Neva river at the Finnish side of the gulf produce heterogeneous current structures that make inverse modelling applications by means of pathway optimisation and fairway design studies illustrative. But seasonal variations of river inflow, solar radiation and wind forcing make stratification and current pattern also highly variable in space and time. To derive conclusive fairway designs that serve all seasons will put the technology here presented to the test.

2.4.1 Drift model based assessments for the Gulf of Finland

Two major patterns can be identified that characterize oil drift in the Gulf of Finland. During winter periods with mainly west- southwesterly winds and summer periods with low winds (figure 3), longshore oil advection at the Finnish coastline is dominant, either driven by winds or riverine transport. Wind and current drift is directed parallel to the coastline or points in offshore direction. Whereas wind drift dominates the winter season, the Neva river outflow is dominant during summer. As a consequence, onshore oil advection at the Finnish coast is reduced and the probability for coastal oil landings is relatively low (figure 6), compared to the values for transition seasons. The values range from below 20% to a maximum of little more than 40% at the northern Finnish and Russian coast, at and east of Finish seaport Kotka. Landing propabilities represent average values of the fraction of the released 1000 particles that are landing on the shore. The figures show spatially integrated values, so that the very near coastal areas might be underrepresented. The distribution of release points favours offshore stations, for the reason that onshore oil propagation is in the focus of the presented study. Offshore regions are well represented with a resolution of $3 \times 22\ km$ at the northern and $6 \times 22\ km$ at the southern side. Across the gulf, propability pattern vary strongly. The lower than 40% propabilities at the Finnish and Northern Russian coast of the Gulf are confronted with generally higher than 50% landing propabilities at the Estonian and southern Russian coast. A broad band of larger than 60% propabilities extends along the southern shoreline of the gulf. In more than half of the cases, a released oil spill is drifting ashore in short time. The average time between oil release at position $X(t)$ and the landing at the shore at time $t + T$, is pictured in figure (4). At the southern shore the average combatting time before a oil spill is reaching the shore is less than 3 days. But moving the release position northwards increases the residence time by days. The residence time is generally larger than 3.5 days and exceeds 5 days in a large domain

starting almost at the entrance of the Gulf at 24.3^oE and extending along the northern shore all the way towards 26.6^oE. This gives an advantage of more than 2 days in oil combatting time by moving a release position across the gulf northwards. As described before, the gain is even heightened by a reduction of the near coastal landing probability from values of >50% to values below 30%.

A second pattern is identified for the transition seasons: spring, late summer and autumn. The monthly mean wind directions change from west-southwest to south-southwest or even south (figure 3) and the dominant wind drift intensifies the onshore oil advection at the northern coast of the gulf. Probability and residence time pattern are reversed. Whereas winter and summer pattern show low values of <30% for the oil landing propability at the norhtern shore of the Gulf of Finland, Spring and Autumn pattern reveal maximum values of more than 50% at nearly identical positions (figure 7). A broad band of low probability values <20% extends along the Estonian coast in upwind direction. The average oil residence time at sea shows similar proportions than the landing probabilities. Where in summer and winter the released oil spent a long times at sea, there it is fastly reaching the coast in autumn and spring (figure 5). Almost everywhere at the Estonian coast, released oil spills spends more than 4 days at sea before they hit the shore, whereas at the Finnish and Norhtern Russian coast oil resides less than 2 days at sea. Compared to winter and summer pattern this is an decrease of more than 3 days at the Finish coast and a comparable increase of about 3 days of oil combatting time off the Estonian coast.

Drift pattern analysis provides us with a set of distinct maps, well suitable for fairway design studies, but it leaves us with the dilemma of which map to choose. The two pattern for summer-winter (SW) and spring-autumn (SA) seasons seems to be equally distributed over the 3 years model period. From 36 month in total, 18 month feature SW pattern and 15 month SA pattern. The remaining 3 month can not be assigned to any pattern. Ambiguities arrise from frequently changing wind conditions and undetermined forcing. The environmental gain of employing one of the two results is difficult to evaluate. SW and SA drift pattern seem to be neither dominant nor significantly overlapping enough to form the background for fairway design decision. Further evaluations have to employ a different method. Demonstration fairways are arranged and evaluated with classical ship routing software. Enviromental and economical gain in terms of travel time and fuel consumption are compared across fairways.

2.4.2 Fairway design evaluations

Fairways are designed to comply with topographical conditions, traffic regulations, national and international agreements and basic economical standards. In the focus of the design process are the vessels operational conditions. Environmental conditions: atmosphere, waves and ocean circulation, that might influence the travel considerable have so far been of minor importance. Printed on a map, fairways consist of as many straight lines as possible and a minimum number of turns. The reason is that ship engines develop maximum operating efficiency under constant conditions, and ship constructions make a course changes tedious and fuel consuming. Instead of continuing the

			Summer/Winter SW		Spring/Autumn SA	
Fairway Design	Destination	Pathlength $\int ds$ [km]	Pathintegral $\int \phi\, ds$ [km]	quotient $\int \phi\, ds / \int ds$	Pathintegral $\int \phi\, ds$ [km]	quotient $\int \phi\, ds / \int ds$
SW(north)	Saint Petersb.	287.1	124.2	0.43	100.1	0.35
SW(south)		288.1	122.2	0.42	101.6	0.35
SA		290.0	80.1	0.28	149.0	0.51
SW	Vyborg	231.6	111.5	0.48	77.5	0.34
SA		243.7	72.2	0.30	124.9	0.51
SW	Ust-Luga	251.1	110.6	0.44	89.2	0.36
SA		253.0	69.0	0.27	134.9	0.53
SW	Sillamäe	224.0	101.3	0.45	96.7	0.43
SA		223.6	57.6	0.26	126.0	0.56

Table 1: Cross-Comparrisson of fairway designs for summer-winter (SW), spring-autumn pattern (SA). Listed are the path length of a fairway, the path integrated cost function ϕ and the normalised path integral of ϕ.

practice of path optimisation of shipping operations with respect to a steady ocean and atmosphere, the Baltic Way project takes a step back and starts with a model based assessment of met.-ocean conditions and transport studies of pollutants. Basic fairway designs are derived by Monte-Carlo techniques with focus on oil combatting time increase and landing propability decrease. Travel distance reduction is imposed by path length optimisation. The basic designs represent indicators on which the specific design process could be based. Ship routing evaluations might serve as a tool for further investigation. To the authors knowledge there has been no attempt to explore the possibility of route evaluations during the planning process of fairways. Neither environmental view points, in terms of pollutant impact reduction, nor economical viewpoints, in terms of fuel and travel time reduction due to ocean circulation employment have been taken into consideration.

Monte-Carlo based fairway optimisations lead to a number of three basic designs. Four harbours were selected for the evaluation: Russias most important oil habour Saint Petersburg, Vyborg, Ust-Luga and Sillamäe. Oil drift pattern for Summer-Winter and Spring-Autumn seasons (discussed in chapter [2.4.1]) are analysed seperately and in a second step combined for a joint analysis. Seasonal ensembles of the cost function ϕ are formed for each release position $\underline{X}$. Ensemble averages are studied for the summer-winter and spring-autumn designs (figure 8, figure 9). Additionally a third pattern was constructed that covers all seasons (figure 10). One way of doing this, is to produce annual averages that cover the complete set of monthly drift pattern. But the result is rather homogeneous and lacks the heterogenity of the seasonal pattern. Unsuitable for the identification of distinct fairways, the annual average pattern have not been studied further. Instead ensemble maxima have been used for the development of fairway designes for all seasons. Ensemble maxima are more prominent and offer larger coverage with substantial cost function values. The constructed annual pattern is therefore applicable to the Monte-Carlo tecnology for fairway optimisations.

Table 1 includes the results of the basic design evaluation. Listed are path length,

Design	Destination	$\int \phi\, ds / \int ds$ SW pattern	$\int \phi\, ds / \int ds$ SA pattern	$\int \phi\, ds / \int ds$ CMB pattern	Ø
SW(north)	Saint Petersburg	0.74	0.60	0.58	0.64
SW(south)		0.72	0.69	0.64	0.68
SA		0.53	0.87	0.69	0.70
CMB		0.74	0.85	0.78	0.79
SW	Vyborg	0.80	0.54	0.55	0.63
SA		0.60	0.86	0.72	0.73
CMB		0.74	0.76	0.80	0.77
SW	Ust-Luga	0.72	0.68	0.65	0.68
SA		0.54	0.89	0.71	0.71
CMB		0.73	0.89	0.80	0.81
SW	Sillamäe	0.76	0.75	0.71	0.74
SA		0.50	0.89	0.72	0.70
CMB		0.75	0.90	0.82	0.82

Table 2: Cross comparrisson of fairway designs for summer-winter (SW), spring-autumn pattern (SA) and combined oil drift pattern (CMB), representing local maxima of the seasonal drift pattern ensemble of the cost function.

path integral of the cost function ϕ and the normalised path integral of ϕ. From the results it seems to be evident that spring-autumn (SA) designs perform little better than summer-winter (SW) designes. Although the gain in choosing a SA design is somewhat reduced by longer pathlenght, it is over-compensated by lower environmental risks. This is expressed by the higher values of the integrated cost function. But the conclusion that SA designs are favourable is somewhat flawed by the fact that their performance is rather low outside the season for which they were designed. Cross examination is a very useful tool for the estimation of the application value of a specific fairway design and it reveals that the SW design performance is better balanced across the seasons. The choice between SW and SA designs is the choice between specialists and all-rounders. The variability of the SA performance is larger, but the cross seasonal difference is low, meaning that in a certain range the annual average performance of SW and SA designs are equal. The difference is generally less than ± 0.01, except for Sillam"ae, where it is 0.06. The combined patten for all seasons and integrated designs perform even better, but represent maximum pattern (i.e. cost function maxima of the drift simulation ensemble). For a more realistic analysis the designs have to be cross examined under equal conditions. Table 2 lists the performance values of seasonal (SW, SA) and combined designs (CMB) for seasonal and combined maximum pattern. It is apparent that combined designes have a better overall performance. In case of Sillamäe and Ust-Luga they perform equally good or even better than the seasonal designs. But it should be remembered that seasonal designes were generated for average pattern and that maximum pattern cover larger areas with more or less equally high values. This suites also the sprin-autumn designs (SA), which perform better than the summer-winter (SW) designes, with the exception of Sillamäe.

In the end it is the choice of the designer to pick one or the other fairway and to choose between alrounders for all seasons or specialist for one season. Average pattern have been

found to be more critical and challenging for the design process than maximum pattern. But latter have the advantage to cover all designs and to make comparrissons possible. Combined all season designes perform best in this comparrisson because seasonal drift features are better covered. But there is no obvious choice without the imperative of a clear design strategy. If a seasonal design should be piced for an all year applications, than it should be SW designs, which performes best across the seasons.

2.5 Wave induced transport of oil

An Oil drift and fate model includes parameterisations of wave effects on oil weathering, i.e. downwards mixing and emulsification which base on wind dependent estimates. Wave induced oil transport has been largely neglected because of the intense computational effort and the wide spread belief that wave induced drift effects are relatively small compared to current and wind drift. But estimates show that the additional drift currents due to wave induced momentum input, i.e. Stokes drift can easily reach the magnitude of the wind and current drift. One-dimensional airy waves $\underline{k} = k \cdot \underline{e}_x$ in $\underline{x}$-direction towards the coast, under shallow water conditions $kh \ll 1$ and $c_g/c_p = 0.5 + kh/sinh(2kh) \approx 1$ (whereas the Taylor expansion $sinh(2kh) = 2kh$ around $kh = 0$ was applied) produce the same magnitude of drift velocity as the wind, when the wave energy gradient $\partial E/\partial x = \rho g/16\ \partial H_S/\partial x$ is equal to the vertical wind induced current shear stress gradient $\partial\tau/\partial z$. For Gulf of Finland model set-up: grid resolution of $0.5' \approx 921m$, surface layer thickness of $3m$ and a drag coefficient of $C_D = 10^{-3}(0.63 + 0.066 \cdot U_{wind}(m/s)^{-1})$, the required wave height change over one grid cell is calculated to be $\Delta H_S = ((3.9 \cdot 10^{-4} + 4.1 \cdot 10^{-5} U_{wind}(m/s) - 1) \cdot U_{wind})^{0.5}$. Wave breaking with a wave height change of $70cm$ produce approximately the same drift velocity as $20m/s$ winds. For $30m/s$ winds the required wave height change over one grid cell is $1.2m$ and for $40m/s$ it is $1.8m$. To elaborate this further, the wind stress equivalent of the wave forcing is studied more in detail for the Gulf of Finland.

Figure (11) shows the spatial distribution of the mean wave induced surface stress, i.e. the magnitude of the wave induced force, that drive the currents. Surface wave and wind stress are treated similarily by the model, and can be compared to each other. For this purpose, the forcing term $\partial_{\underline{x}} \cdot \underline{\underline{S}} + \partial_z \tau(U_{wind})$, where $\underline{\underline{S}}$ represents the wave radiation stress tensor (13), is rewritten to a function for U_{wind} in case of a balance of forces. The result shows the magnitude of the wave induced forcing in terms of the wind speed, i.e. the winds that would be required to drive the same currents as the waves. Pictured (11) is a average value for the years 1991 to 1994. Local maxima at near coastal locations represent a average driving force that would balance $17m/s$ wind. In case of a strong storms, like the 2005 winter event (Soomere et al. [2008], $37.5m/s$ measured in Estonia), the wind equivalent of the wave induced surface stress increases signifficantly and might locally reach values of $25m/s$. The spatial distribution of wave affected regions is rather independent of the actual wind strength and remains unchanged. Looking at the results, one should keep in mind that they dependent strongly on the model set-up, for the reason that gradients are compared. Figure (11) illustrates that near coastal wave effects might

locally have significance for onshore oil transport and can not be ignored. This is even more the case because topographically steered currents propagate pollutants along the shore, whereas wind waves are refracted and often act in perpendicular direction to the coastline.

Published studies focus on scenarios, shipping accidents and storm cases. Systematic wave studies have been prevented by computational effort. This is especially true for calm conditions with swell. The present study focuses on the analysis of magnitude and seasonal variation of wave induced drift effects under different weather conditions. More than 50000 drift simulations at 528 stations were conducted in the Gulf of Finland to estimate average effects of waves on the transport pattern of oil at sea. The simulations cover the year 1992, which represents an average year. Unlike the fairway design studies, where at least 3 years of data were covered, the here presented analysis will not investigate the seasonality of the wave induced oil drift effects. The simulation period is to short to analyse drift pattern on sub-annual scale. Instead average wave effects are studied. Additionally scenario studies for the January 2005 storm event have been evaluated to estimate maximum wave transport effects.

2.5.1 Introduction into the basics of wave-current interactions

In the following, a constructive approach is used to derive time averaged interaction equations of ocean waves and currents using perturbation theory. Wave dependent primitive equations for momentum and transport are derived and wave dependent energy equations are constructed. This approach follows the application in this chapter, which deals with drift simulations. The state vector (horizontal-, vertical currents, position, water depth)=$(\underline{u}, w, x, h)^T$ is expanded into a series of harmonic polynomes representing the undisturbed solution, linear waves and higher order components. These solutions are understood as perturbation modes of 0-th, 1-th and 2-nd order. The phase averaged equations describe the evolution of the slowly varying, wave dependent mean state. This requires the introduction of a scale separation, although this does not become explicitly apparent in this chapter. Wave amplitude- and phase dynamics are considered to take place at different scales, typically associated with the slowly varying currents and the fastly changing wave spectra. The equations are developed to the lowest non-linear, the 2-nd order, to include the effect of the Stoke's drift. The perturbation modes are Taylor polynomes of the general solution (3) and (4) (shallow water waves)

$$(\underline{u}, w, \underline{x}, h) = \left(\underline{u}^0, w^0, \underline{x}^0, h^0\right) + (\delta\underline{u}(\underline{x}, t), \delta w(\underline{x}, t), \delta\underline{x}, \delta h(\underline{x}, t)) \quad (3)$$

$$(\delta\underline{u}, \delta w, \delta x, \delta h) = \left(\frac{\partial(\cdot)}{\partial x}, \frac{\partial(\cdot)}{\partial z}, \int \frac{\partial(\cdot)}{\partial x} dt, \int \frac{\partial(\cdot)}{\partial z} dt\right) \frac{\omega}{k} \frac{cosh(kh(\underline{x}, z, t))}{sinh(kD)} a\ sin\theta \quad (4)$$

of the horizontal velocity component $\underline{u}$, evaluated at the stationary state $(\underline{u}^0, w^0, \underline{x}^0, h^0)$ is given by

$$\underline{u} = \underline{u}^0 + \delta\underline{u}|_{h=h^0} + \frac{\partial\delta\underline{u}}{\partial\underline{x}}|_{h=h^0} \cdot \delta\underline{x} + \frac{\partial\delta\underline{u}}{\partial z}|_{h=h^0}\delta z + \ldots \quad (5)$$

$$\underline{u} \;=\; \underline{u}^0 + \omega a \frac{cosh(kh^0)}{sinh(kD)} cos\theta + \omega k a^2 \frac{cosh^2(kh^0)\; sin^2\theta + sinh^2(kh^0)\; cos^2\theta}{sinh^2(kD)} + \ldots, \quad (6)$$

whereas the right hand side of equation (4) includes derivatives and integrals of the velocity potential $\Phi(\underline{x}, z, t)$. Please note that equation (4) characterises nonlinear waves, because the depth scaling function $cosh(kh)/sinh(kD)$ is not a constant, but depends on the wave field. The two equations (3) and (4) describe waves that are propagating in $\underline{x}$ direction along layers of constant depth $h = D+z$, with $z = 0$ at the surface and z=-D at the sea bed. For a given configuration, waves of amplitude $a(\underline{x}, t)$ and phase $\theta = \underline{k}\cdot\underline{x} - \omega t$ propagate along characteristics $\underline{c}_g = \partial\omega/\partial\underline{k}$ and $\dot{\underline{k}} = -\nabla\omega$, as specified by the dispersion relation $\omega = (gk\; tanh(kh))^{0.5} + \underline{k}\cdot\underline{u}$. The first two terms on the right hand side of (5) characterise Eularian currents and linear waves, whereas the last two terms, after phase averaging over θ ($0 \le \theta \le 2\pi$), describe the Stoke's drift $u_{sd} = \omega k a^2/(2sinh^2 kD)$.

To derive a prognostic equation for the mean current, as sum of Eularian current u^0 and wave induced Stoke's drift u_{sd}, the Taylor term (6) is applied to the momentum equation $d\underline{u}(t, \underline{x}(t))/dt = \underline{F}$. Here d/dt denotes total derivatives and $\underline{F}$ is the sum of external forces and body forces. The equation is derived under the condition of incompressibility, which filters out most of all sound waves. To ensure incompressibility and to balance the periodic wave motion, a pressure gradient term $\nabla\delta p$ is added to the momentum equation, which takes the form $d\underline{u}/dt = \underline{F} - \nabla\delta p$. Every perturbation of the Eularian semi-equilibrium state $\underline{u}^0$, which is assumed to be locally homogeneous and static on the spatial and temporal scales associated with the wave field, generates a perturbation in the pressure field according to Bernoulli's formula (7). The pressure contribution is calculated by integration of δp in a vertical with the wave motion co-moving frame. This requires a transformation of the integral, whereas the volume element takes the form $dx\; dy\; d\zeta = dz/D$ (with $\zeta = 0$ at the surface and $\zeta = -1$ at the ground) and the only transformation matrix element that differs from identity is $T_{zz} = \partial_\zeta \delta h(\zeta) = \delta\underline{u}\; kD/\omega$. Using the relation $c_g/c_p = 0.5 + kh^0/sinh(2kh^0)$ for the wave group- to phase velocity ratio: $c_g = \partial_k\omega$ to $c_p = \omega/k$, the momentum contribution due to wave related pressure variations takes the form of (8).

$$\int_{z_1}^{z_2} \delta p\; dz \;=\; -\int_{z_1}^{z_2} \left(\rho\frac{\delta\Phi}{\delta t} + \rho g\delta h\right)\; dz = \int_{z_1}^{z_2} \rho\left(\frac{\omega}{k} - \frac{g}{\omega} tanh(kh^0)\right)\delta\underline{u}\; dz \quad (7)$$

$$= \; kD \int_{\zeta(z_1)}^{\zeta(z_2)} \left[\rho g \frac{c_g}{c_p} \frac{4\; cosh^2\; kD(1+\zeta)}{sinh\; 2kD + 2kD} \left(1 - \frac{tanh\; kD(1+\zeta)}{tahh\; kD}\right) a^2 cos^2\theta\right] d\zeta \quad (8)$$

Similarily, the advective wave momentum contribution to the mean flow is handled. The momentum balance equation is rewritten to a partial equation and the continuity equation for incompressible flows is used to eliminate divergence terms of the flow field $\nabla\cdot\underline{u} = 0$. The advective terms (9) can be simplified through Taylor expansion of $\underline{u}$ (using (6)) and averaging the results over the phase $0 \le \theta \le 2\pi$ of the wave field

$\langle\cdot\rangle = 1/2\pi \int_0^{2\pi}(\cdot)d\theta$.

$$\frac{d\underline{u}(t,\underline{x}(t))}{dt} = \frac{\partial \underline{u}}{\partial t} + \underline{u}\cdot\frac{\partial \underline{u}}{\partial \underline{x}} = \frac{\partial \underline{u}}{\partial t} + \frac{\partial(\underline{u}\otimes\underline{u})}{\partial \underline{x}} \tag{9}$$

$$\frac{d\,\langle\underline{u}(t,\underline{x}(t))\rangle}{dt} = \frac{\partial\left(\underline{u}^0+\underline{u}_{sd}\right)}{\partial t} + \frac{\partial\left(\left(\underline{u}^0+\underline{u}_{sd}\right)\otimes\left(\underline{u}^0+\underline{u}_{sd}\right)\right)}{\partial \underline{x}} + \frac{\partial\,\langle\delta\underline{u}\otimes\delta\underline{u}\rangle}{\partial \underline{x}} \tag{10}$$

Equation (10) includes time derivatives of the mean velocity $\underline{u}^0+\underline{u}_{sd}$ and the divergence of the tensor product $\delta\underline{u}\otimes\delta\underline{u}$. All other terms can be omitted, because the phase average of $\delta\underline{u}$ over periods of $[0,2\pi]$ is nil. The last term of (10) corresponds to the wave related mean momentum input due to the self-correlation of the flow field. It is calculated to

$$\int_{z_1}^{z_2}\delta\underline{u}\otimes\delta\underline{u}\;dz = \int_{z_1}^{z_2}\frac{\underline{k}\otimes\underline{k}}{k}g\frac{c_g}{c_p}\frac{4\;cosh^2kh}{sinh\;2kD+2dD}\;a^2cos^2\theta\;dz \tag{11}$$

Collecting all tems provides the following result:

$$\frac{\partial\,\langle\underline{u}\rangle}{\partial t} = \langle\underline{F}\rangle - \langle\underline{u}\rangle\cdot\frac{\partial\,\langle\underline{u}\rangle}{\partial\underline{x}} - \frac{\partial}{\partial\underline{x}}\cdot\underline{\underline{S}} \quad \text{with} \quad \langle\underline{u}\rangle = \underline{u}^0+\underline{u}_{sd} \quad \text{and} \tag{12}$$

$$\underline{\underline{S}} = \frac{1}{2\pi}\int_0^{2\pi}\int_{\zeta(z_1)}^{\zeta(z_2)}\left(\delta\underline{u}\otimes\delta\underline{u}+\underline{\underline{\delta}}\delta p\right)\;d\zeta\;d\theta \tag{13}$$

$$= E\left(\frac{c_g}{c_p}\left[\frac{\underline{k}\otimes\underline{k}}{k^2}+\underline{\underline{\delta}}\right]\frac{sinh\;2kh+2kh}{sinh\;2kD+2kD} - \underline{\underline{\delta}}\,\frac{cosh\;2kh}{4\;sinh^2\;kD}\right), \tag{14}$$

Here $\underline{\underline{S}}$ denotes the radiation stress tensor, $E = 1/2\;ga^2$ is the wave energy, $h = D(1+\zeta)$ is the local depth of layer ζ and $\underline{\underline{\delta}}$ is the Kronecker's delta. Please note that deriving (14) from (13), the vertical integral of the tensor product $\delta\underline{u}\otimes\delta\underline{u}$ over depths $\zeta(z_1)$ to $\zeta(z_2)$ was replaced by the static integral over depths z_1 to z_2. The introduced error is of third order and negligible. Keeping in mind that only integrals of non-linear terms in the limits of z_1 to z_2 contribute to the wave impetus, it becomes appearent that the only non-vanishing contribution to the hydrodynamic transport equations is the radiation stress divergence in the momentum equation. Doing so, the state vector changes from the Eularian vector $(\underline{u}^0,w,x,h)^T$ to the mean state $(\langle\underline{u}\rangle = \underline{u}^0+\underline{u}_{sd},w,x,h)^T$. Turbulent mixing and nonlinear dissipation has been excluded from these considerations.

The wave energy equation is easily constructed from the momentum equation $d\underline{u}/dt = \underline{F} - \nabla\cdot\underline{\underline{S}}$ by scalar multiplication from the right with the velocity vector $\underline{u}$ and following phase averaging. The outcome is a prognostic equation for the kinetic energy $E_{kin} = \frac{1}{2}\,\langle\underline{u}^2\rangle$ of which the waves contribution is $E_{kin} = \frac{1}{2}\,\langle\delta\underline{u}^2\rangle$. Its derivation makes use of the identity $\partial_{(\underline{x},t)}\underline{u}\cdot\underline{u} = \frac{1}{2}\partial_{(\underline{x},t)}\underline{u}^2$, where $\partial_{(\underline{x},t)}$ denotes partial derivatives with respect to $\underline{x}$ or t.

$$\frac{\partial E_{kin}}{\partial t} = \langle\underline{F}\rangle\cdot\langle\underline{u}\rangle - \langle\underline{u}\rangle\cdot\frac{\partial E_{kin}}{\partial\underline{x}} - \frac{\partial}{\partial\underline{x}}\cdot\underline{\underline{S}}\cdot\langle\underline{u}\rangle \tag{15}$$

For reasons of simplicity, at the derivation of the right hand side of equation (15), the average of products has been replaced by the product of averages. Convenient terms for the potential energy can be constructed from the continuity equation. The radiation stress appears as a sink term on the right-hand side of the equation (15). Its contribution is closely linked to the wave energy gradient and thereby to the amount of energy that is dissipated through wave breaking. Its effect is illustrative pictured by waves right at the shore, where the remaining part of the wave energy is finally removed and a beach walker experiences upwards running gushs of sea water that might reach his position. In wave modeling this effect is rarely considered. Instead, empirical formula are used to describe the energy dissipation due to wave breaking and wave-current interaction.

2.5.2 Wave studies: Methodology and Results

Wave induced momentum and transport assessments often estimate the Stoke's drift diagnostically and add it to the Eularian currents. Spectral integrated wave parameters: significant wave height, period and direction, are employed to calculate representative values of wave number and energy, and finally to calculate the Stoke's drift itself. We refrain from such a practice and use instead a coupled ocean wave and circulation model to calculate the wave dependent drift currents. For applications in regions with low tides and average surges, e.g. Baltic Sea and Gulf of Finland, a one-way coupled system can be applied, in which the wave model is feeding the circulation model. The wave induced momentum contribution to the drift currents is implemented as additional force at the surface, that drives the mean flow. Wind and wave forcing is combined into one term $\partial\tau/\partial z - \partial\underline{\underline{S}}/\partial\underline{x}$, in which $\underline{\underline{S}}$ denotes the radiation stress tensor.

The results show that oil residence times in near coastal waters already under average conditions differ considerably from classical results, when wave induced transport is considered. The model results show local time differences of -2.2 days to 1.3 day (figure 13). The effects are very localised. Close to the coast, around islands and in the middle of the Gulf at around 26^oE and close to the entrance are the largest differences. The latter are associated with considerable depth gradients at open sea, wave refraction and eventually wave induced momentum generation in the direction of the wave energy gradient (figure 11, 12). At the lee-side of islands, the wave energy gradients are caused by the shadowing effects. There, the wave impact has a focussing effect, bringing lee-side approaching pollutants on land track. In opposite direction, waves have a diverging effect, causing pollutants to stay longer offshore. At the surf zone and close to the shoreline, the wave induced currents are following the depth gradient and might produce coastal jets. Depending on the direction of pollutant transport and the angle of the waves towards the coast, the jets might prevent onshore oil propagation or further it. Waves excert accelerating forces on the currents and change the drift pattern. The average effect is noticeable everywhere in the Gulf and amounts to $\pm 10\%$ landing probability (14).

Oil propagation and weathering studies show the locally strong impact of waves on oil at sea. The open question that remains is, how does this affect the fairway designs. Although fairway designs are not meeting the here presented considerations,

they naturally avoid the vicinity of islands and coastal nearshore regions. With that they avoid the most critical zones. A closer evaluation of the wave induced drift characteristic along presented fairways and impact assessments of waves on the fairway performance have not been part of the programe.

2.6 Apendix1: Circulation model

DMI runs operationally a three-dimensional, free-surface, baroclinic ocean circulation and sea ice model that solves the primitive equations for horizontal momentum and mass, and budget equations for salinity and heat on a spherical, with the earth rotation co-moving grid. The circulation model was originally developed by the Federal Maritime and Hydrographic Agency (BSH) in Hamburg and has been applied to the North Sea and Baltic Sea since the early 1990'ies (Kleine et al. [1994], Dick et al. [2001]). The vertical transport assumes hydrostatic balance and incompressibility of sea water, i.e. divergence free current velocity fields. Horizontal transport is modelled using Boussinesq approximation, where density differences are neglected in all but gravity terms. Higher order contributions to the physical dynamics are parameterized following Smagorinsky [1963] in the horizontal, and using a $k-\omega$ turbulence closure and mixing scheme, which has been extended for buoyancy affected geophysical flows (Umlauf et al. [2003]) in the vertical. The turbulence scheme includes parameterisation of breaking surface and internal waves. Stability functions from Canuto et. al. [2001, 2002] for the vertical eddy diffusivities of salinity, temperature and momentum have been applied. The numerical implementation uses staggered Arakava-C grid and z-level coordinates, flux corrected horizontal advection scheme and no-slip conditions along coastlines. Boundary conditions at sea surface and sea bed use quadratic velocity dependent formulations of the wind induced shear-stress and frictional bottom stress. Following Oleg Andrejev et al. [2004] the wind drag coefficient was set to $C_D = 0.001 \cdot (0.63 + 0.066 \cdot \bar{U}_{wind} \cdot (s/m))$, where $\bar{U}_{wind}$ is the wind speed. Unrealistic strong wind forcing during storms is avoided by making the wind stress parameterisation dependent on the effective wind velocity in relation to the current velocity. At the sea bed, a constant friction coefficient $R = 0.0021$ has been applied. The model is two-way coupled with a Hibler type sea ice model [1979], treating both its dynamics and thermodynamics ([1994, 2001]). To account for penetration of short wave radiation into the subsurface model layers a proper parameterisation of the insolation suited for the Baltic Sea (Meier, [2001] 2001) was implemented.

2.7 Glossary

T	Time spent at sea (residence time in water)
$TM = 10days$	Runtime of the oil drift simulations
X	Oil release position
T	Time
$\underline{x}(t)$	Position in space
$NL(\underline{X})$	Number of oil landings
$NT = 1000$	Total number of released particles per release

2.8 Figures

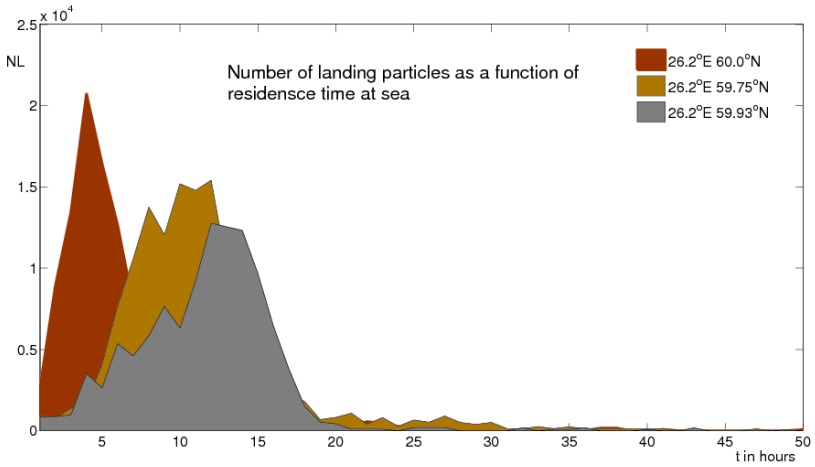

Figure 2: Histogram of residence times of oil particles at sea at three positions: 60.0^oN (brown), 59.75^oN (ochre), 59.93^oN (gray) of longitude 26.2^oE.

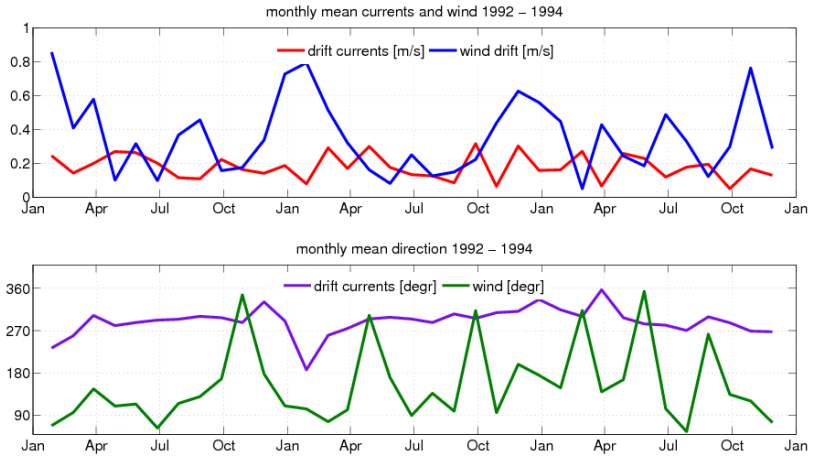

Figure 3: Monthly mean wind drift $0.03 \cdot \underline{U}_{wind}$ (top, blue), current velocity (top, red) and direction of the mean currents (magenta), winds (green) for the years 1992 to 1994.

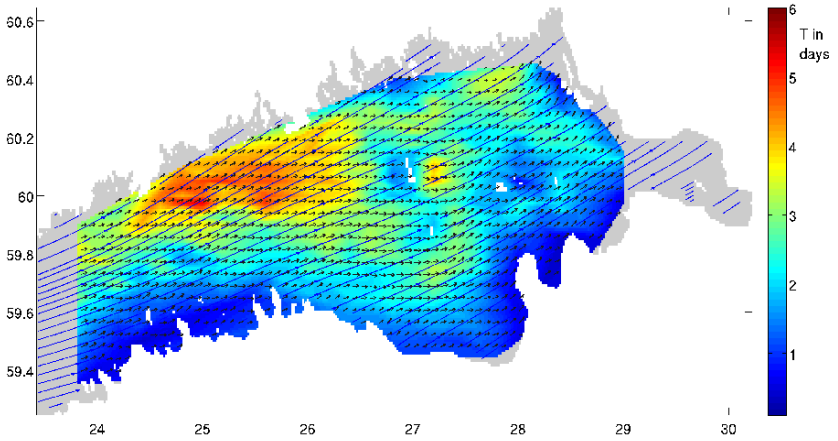

Figure 4: Spatial distribution of average oil residence time at sea (color), streamlines of average $10m$ winds U_{wind} and vector plots of drift currents (sum of wind drift $0.035 \cdot U_{wind}$ and ocean currents for summer, winter month (left) and transition seasons (right)(1992-1994)

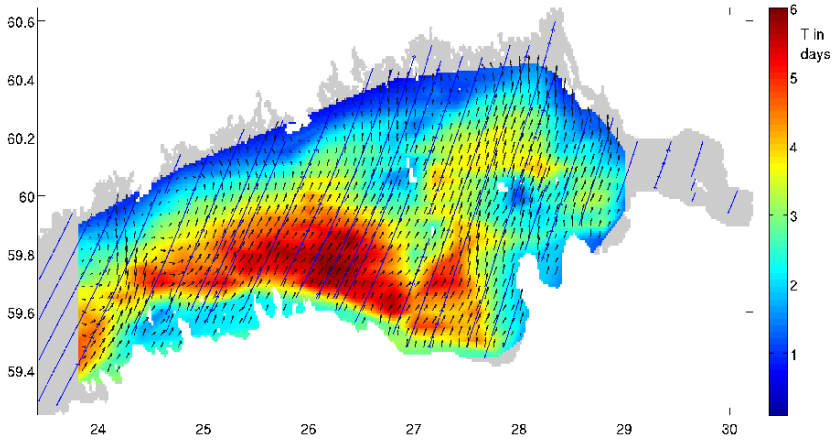

Figure 5: Spatial distribution of average oil residence time at sea (color), streamlines of average $10m$ winds U_{wind} and vector plots of drift currents (sum of wind drift $0.035 \cdot \underline{U}_{wind}$ and ocean currents for spring, autumn month (1992-1994)

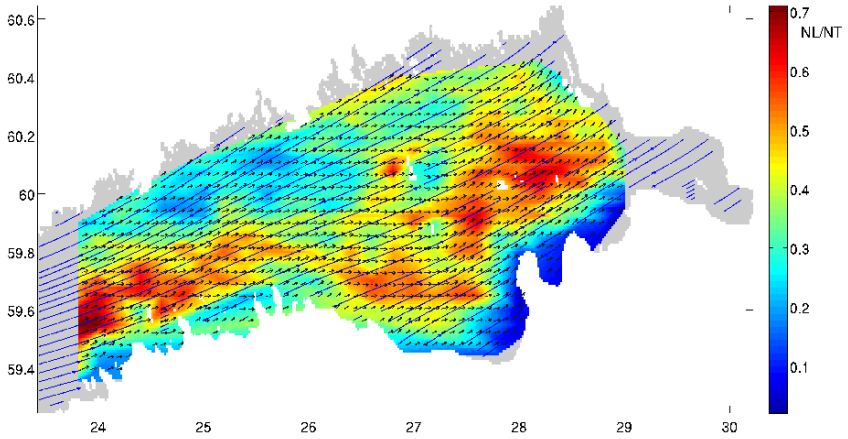

Figure 6: Spatial distribution of coastal hit probability (color), streamlines of average $10m$ winds U_{wind} and vector plots of drift currents (sum of wind drift $0.035 \cdot \underline{U}_{wind}$ and ocean currents for summer, winter month (1992-1994)

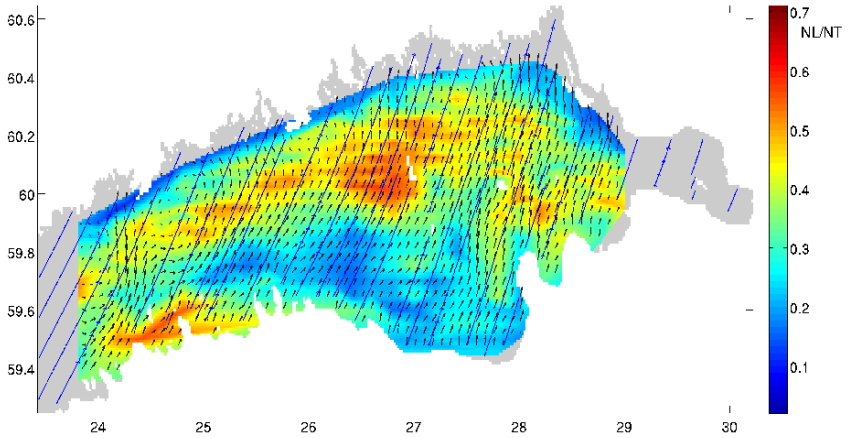

Figure 7: Spatial distribution of coastal hit probability (color), streamlines of average $10m$ winds U_{wind} and vector plots of drift currents (sum of wind drift $0.035 \cdot \underline{U}_{wind}$ and ocean currents for spring, autumn month (1992-1994)

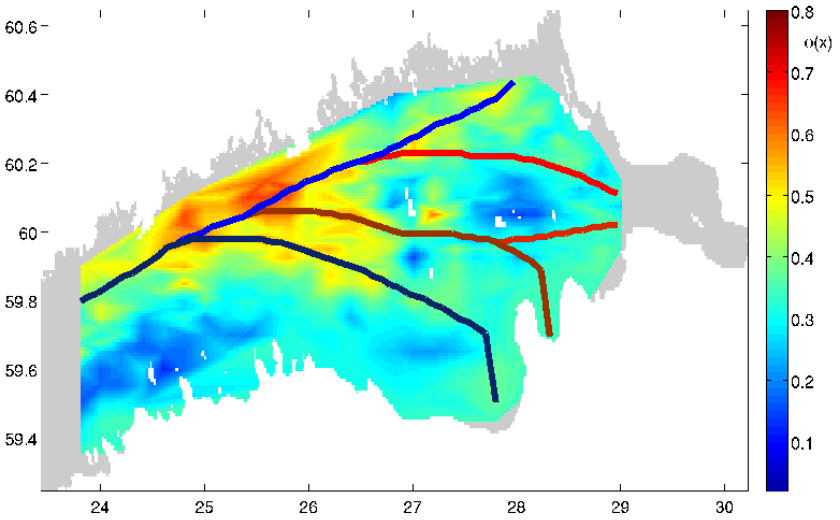

Figure 8: Path optimised summer-winter fairway design for routes to Vyborg, Saint Petersburg, Ust-Luga and Sillamäe corresponding to cost function ϕ maxima, i.e. minima of coastal hit propability and maxima of oil combating time.

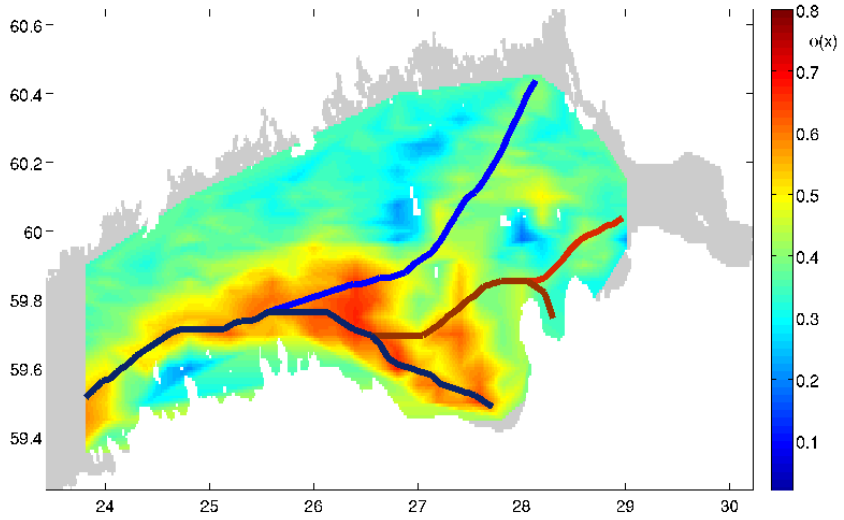

Figure 9: Path optimised spring-autumn fairway design for routes to Vyborg, Saint Petersburg, Ust-Luga and Sillamäe corresponding to cost function ϕ maxima, i.e. minima of coastal hit propability and maxima of oil combating time.

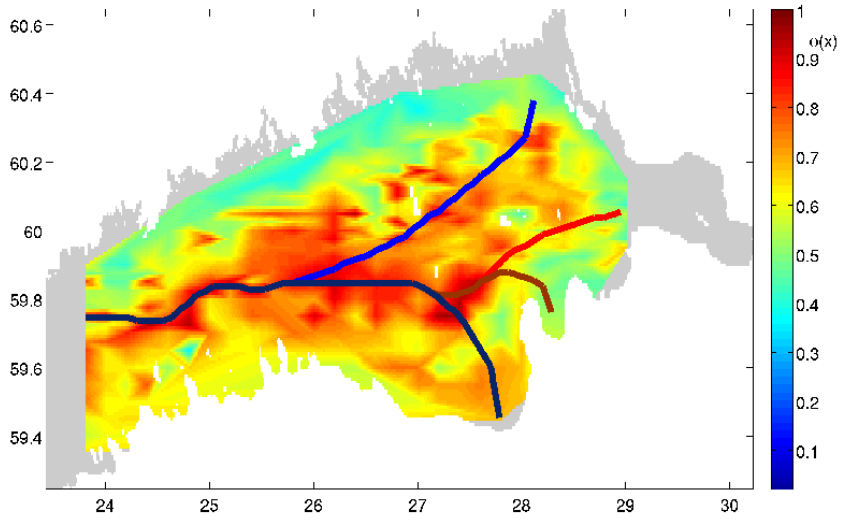

Figure 10: Path optimised summer-winter fairway design for routes to Vyborg, Saint Petersburg, Ust-Luga and Sillamäe corresponding to coast function ϕ maxima, i.e. minima of coastal hit probability and maxima of oil combating time.

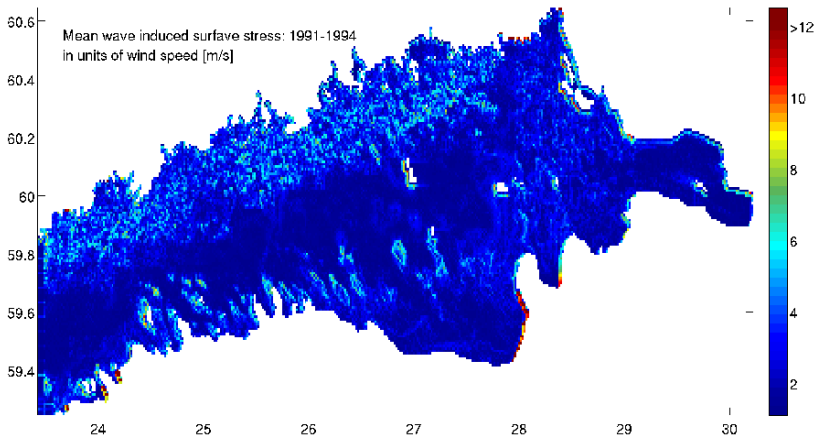

Figure 11: Mean wave induced surface stress 1991-1994 in units of wind speed, i.e. sollutions of the discretised equation $\Delta/\Delta\underline{x}$(wave-stress)$= -\Delta/\Delta z$(wind-stress) with $\Delta\underline{x} \approx 921m$ and $\Delta z = 3m$.

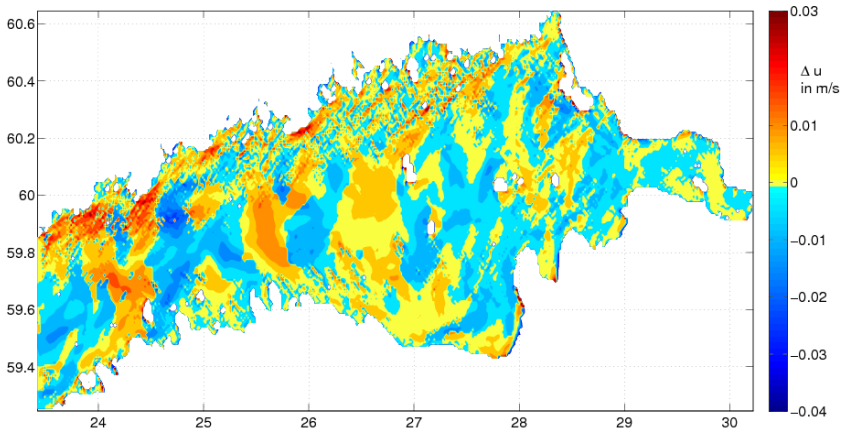

Figure 12: Anual mean current velocity difference (magnitude) 1992 with and without waves $\underline{u}$(waves)-$\underline{u}$(no-waves). Positive/Negative are magnitudes of difference currents in Norherly/Southerly direction.

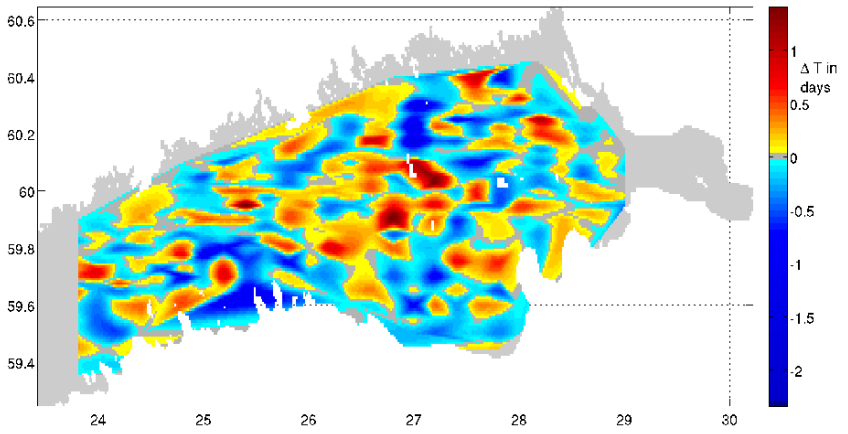

Figure 13: Anual mean oil residence time difference 1992 with and without waves T_{res}(waves)-T_{res}(no-waves).

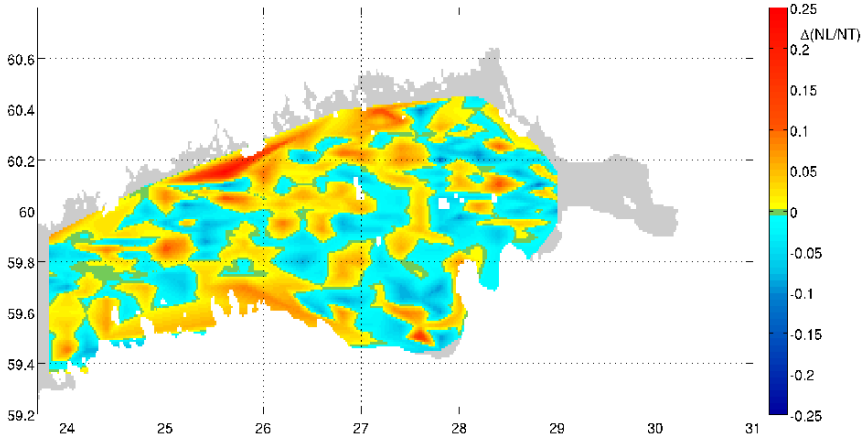

Figure 14: Difference of annual mean oil landing probabilities at the coast with and without waves for the year 1992.

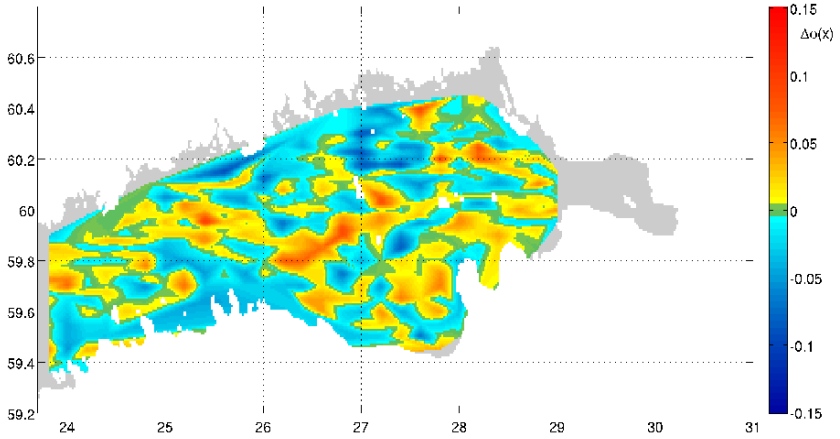

Figure 15: Difference of annual mean cost function at the coast with and without waves for the year 1992.

References

[2004] Andrejev, O., K. Myrberg, P. Alenius, P.A. Lundberg, 2004: "Mean circulation and water exchange in the gulf of Finland-a study based on three-dimensional modelling", Boreal Environment Res. Vol 9, pp.1-16

[2011] Andrejev O., Soomere T., Sokolov A., Myrberg K., 2011. "The role of spatial resolution of a three-dimensional hydrodynamic model for marine transport risk assessment", Oceanologia, 53 (1-TI), 309–334

[1980] Audunson, T.,1980: "The fate and weathering of surface oil from Bravo blowout.", Marine Environ. Res. Vol 3, pp.35-61

[1994] Kleine E., 1994: "Das operationelle Modell des BSH für Nordsee und Ostsee, Konzeption und Übersicht.", Federal Maritime and Hydrographic Agency (BSH), Hamburg, Technical Report, 126pp

[2001] Dick, S., E. Kleine, S.H. Mueller-Navarra, H. Kleine, H. Komo, 2001: "The Operational Circulation Model of BSH (BSHcmod)-Model description and validation", Berichte des BSH 29/2001, Federal Maritime and Hydrographic Agency (BSH), Hamburg, 48pp.

[1990] Stephan Dick, Kai Christian Soetje, 1990: "An operational oil dispersion model for the German Bight", Deutsche Hydrographische Zeitschrift DHZ, Ergänzungsheft, Reihe A, Nr.16, ISSN 0070-4164

[1993] Børresen J.A., 1993: "Olje på havet." Gyldendal.

[1976] Bergström, S., 1976: "Development and application of a conceptual runoff model for Scandinavian catchments", SMHI Reports RHO, No. 7, Norrköping

[1992] Bergström, S., 1992: "The HBV model - its structure and applications", SMHI Reports RH, No. 4, Norrköping

[2001] Canuto, V.M., A. Howard, Y. Cheng, M.S. Dubrovikov, 2001: "Ocean Turbulence. Part I: One-point closure model-momentum and heat vertical diffusivities", J. Phys Ocean. 31, pp.1413-1426

[2002] Canuto, V.M., A. Howard, Y. Cheng, M.S. Dubrovikov, 2002: "Ocean Turbulence. Part II: Vertical diffusivities of Momentum, Heat, Salt, Mass and Passive Scalars", J. Phys Ocean. 32, pp.240-264

[2006] Christensen, O. B., M. Drews, J. H. Christensen, K. Dethloff, K. Ketelsen, I. Hebestadt, and A. Rinke, 2006: "The HIRHAM Regional Climate Model. Version 5, DMI technical report No. 06-17", Available at http://www.dmi.dk/dmi/tr06-17.pdf

[2003] B.M. Christiansen, 2003: "3D Oil Drift and Fate Forecasts at DMI." Tech. Rep. No. 03-36, Danish Meteorological Institute, Denmark.

[1984] Dippner, J.W., 1984: "Ein Strömungs- und Öldriftmodel für die Deutsche Bucht.", Veröff. Inst. Meeresforsch. Bremerhaven, Suppl. B.8, 188 S.

[1969] Fay, J.A., 1969: "The spread of oil slicks on a calm sea.", Oil on the Sea, ed. D.P. Hoult, pp.53-63

[1971] Fay, J.A., 1971: "Physical processes in the spread of oil on a water surface.", Proc. of Joint Conf. On Prevent. and Control of Oil Spills, USA-Washington, D.C., June 15-17, 1971, pp. 463-467

[1971] Forrester, W.D., 1971: "Distribution of suspended oil particles following the grounding of the tanker Arrow", J. Of marine research, 29, pp.151-170

[1979] Hibler, W.D. III, 1979: "A dynamic thermodynamic sea ice model", J. Phys. Ocean. 9, pp. 815-846

[1982] Johansen, Ø., 1982: "Drift of submerged oil at sea", Continental Shelf Institute Report No. P 319/1, Trondheim p51

[2005] Johansen, Ø. et al., 2005: "Simulations of oil drift and spreading and oil spill response analysis", Work page 4 of project Arctic Operational Platform (ARCOP).

[1975] Leibovich, S, 1975: "A natural limit to the containment and removal of oil spills at sea", ocean Engng, Vol3, pp29-36

[1982] Mackay, D., W.Y. Shiu, K. Hossain, W. Stiver, D. McCurdy, S. Paterson, P. Tebeau, 1982: "Development and calibration of an oil spill behaviour model". U.S. Coast Guard Dept. Of Chemical Engng. And Appl. Chem. 69p

[1983] Mackay, D., W. Stiver, P. A. Tebeau, 1983: "Testing of crude oils and petroleum products for environmental purposes." Proc.1983 Oil Spill Conf., pp. 331-337

[2001] Meier, H. E. M., 2001: "On the parameterisation of mixing in three-dimensional Baltic Sea models." J. Geophys. Res. 106, C12, 30997-31016

[2011] Oleg Andrejev, Tarmo soomere, Alexander Sokolov, Kai Myrberg, 2011: "The role of spatial resolution of a three-dimensional hydrodynamic model for marine transport risk assessment", OCEANOLOGIA, 53, pp 309-334

[1985] Pahlke, H., 1985: "Physikalische grundlagen der mechanischen Ölbehandlung. Teil 3: Verhalten von Öllachen auf Wasser.", Umweltforschungsplan des Bundesministers des Inneren, Forschungsbericht 10203 204/01, 185 p

[2005] Pikkarainen A.-L. and P. Lemponen, 2005: "Petroleum hydrocarbon concentrations in Baltic Sea subsurface water.", Boreal Environment Research, 10, 125-34.

[1989] Reed, M., 1989: "The physical fates component of the CERCLA Type A model system.", oil and Chemical Pollution 5, pp 99-124

[1993] Reed, M.,P.S. Daling, P.J. Brandvik, I. Singsaas, 1993: "Laboratory tests, experimental oil spills, models and reality: the Braer oil Spill." In: Proceedings of the 16-th arctic and Marine Oil Spill Program Technical Seminar, Environment, Canada, pp.203-209

[1994] Reed, M., O.M. Aamo, 1994: "Real time oil spill forecasting during an experimental oil spill in the Arctic ice.", Spill Science and Technology Bulletin 5(1), pp 203-109

[1999] Reed, M. et. al, 1999: "Oil spill modelling towards the close of the 20th century: Overview of the state of the art.", Spill Science & Technology Bulletin Vol. 5, No. 1, pp 3-16.

[1963] Smagorinsky, J., 1963: "General circulation experiments with primitive equations, 1. The basic experiment.", Mon. Wea. Rev. 91, pp 99-164

[2008] Soomere, T., A. Behrens, L. Tuomi, J.W. Nielsen, 2008: "Wave conditions in the Baltic Proper and in the Gulf of Finland during windstorm Gudrun", Nat. Hazards Earth Syst. Sci., 8, pp. 37-46

[2010] Soomere, T.; Viikmäe, B.; Delpeche, N., and Myrberg, K., 2010. "Towards identification of areas of reduced risk in the Gulf of Finland, the Baltic Sea." Proceedings of the Estonian Academy of Sciences, 59 (2), 156–165.

[2011a] Soomere, T.; Delpeche, N.; Viikmäe, B.; Quak, E.; Meier, H.E.M., and Döös, K., 2011a. "Patterns of current-induced transport in the surface layer of the Gulf of Finland." Boreal Environment Research, 16 (1), 1–23.

[2011b] Soomere, T.; Andrejev, O.; Sokolov, A., and E. Quak, E., 2011b. "Management of coastal pollution by means of smart placement of human activities." Journal of Coastal Research, Special Issue No. 64, 951–955.

[2011c] Soomere T.; Andrejev O.; Sokolov A., and Myrberg K., 2011c. The use of Lagrangian trajectories for identification the environmentally safe fairway. Marine Pollut. Bull., 62 (7), 1410–142.

[2011d] Soomere, T.; Berezovski, M.; Quak, E., and Viikmäe, B., 2011d. "Modeling environmentally friendly fairways using Lagrangian trajectories: a case study for the Gulf of Finland, the Baltic Sea." Ocean Dynamics, 61 (10), 1669–1680.

[1998] Sørensen J.H., 1998: Sensitivity of the DERMA long-range Gaussian dispersion model to meteorological input and diffusion parameters. Atmospheric Environment Vol. 32, No. 24, pp 4195-4206.

[2007] Sørensen, J.H. et al., 2007: The Danish emergency response model of the atmosphere (DERMA). J. of Environmental Radioactivity 96, pp 122-129.

[1942] Sverdrup, H.U., M.W. Johnson, R.H. Fleming, 1942: "The oceans", prentice-Hall, new York, pp. 481-482

[2003] Umlauf L., H. Burchard, K. Hutter, 2003: "Extending the $k-\omega$ turbulence model towards oceanic applications", Ocean Modelling 5: pp.195-218

[2012] Xi L., Soomere T., Stanev E., Murawski J., "Event driven approach for the identification of the environmentally safe fairway in the south-western Baltic Sea and Kattegat", submitted to Ocean Dynamics